Cell Reports, Volume *40*

Supplemental information

BET inhibition induces vulnerability to MCL1 targeting through upregulation of fatty acid synthesis pathway in breast cancer

Gonghong Yan, Augustin Luna, Heping Wang, Behnaz Bozorgui, Xubin Li, Maga Sanchez, Zeynep Dereli, Nermin Kahraman, Goknur Kara, Xiaohua Chen, Caishang Zheng, Daniel McGrail, Nidhi Sahni, Yiling Lu, Ozgun Babur, Murat Cokol, Bora Lim, Bulent Ozpolat, Chris Sander, Gordon B. Mills, and Anil Korkut

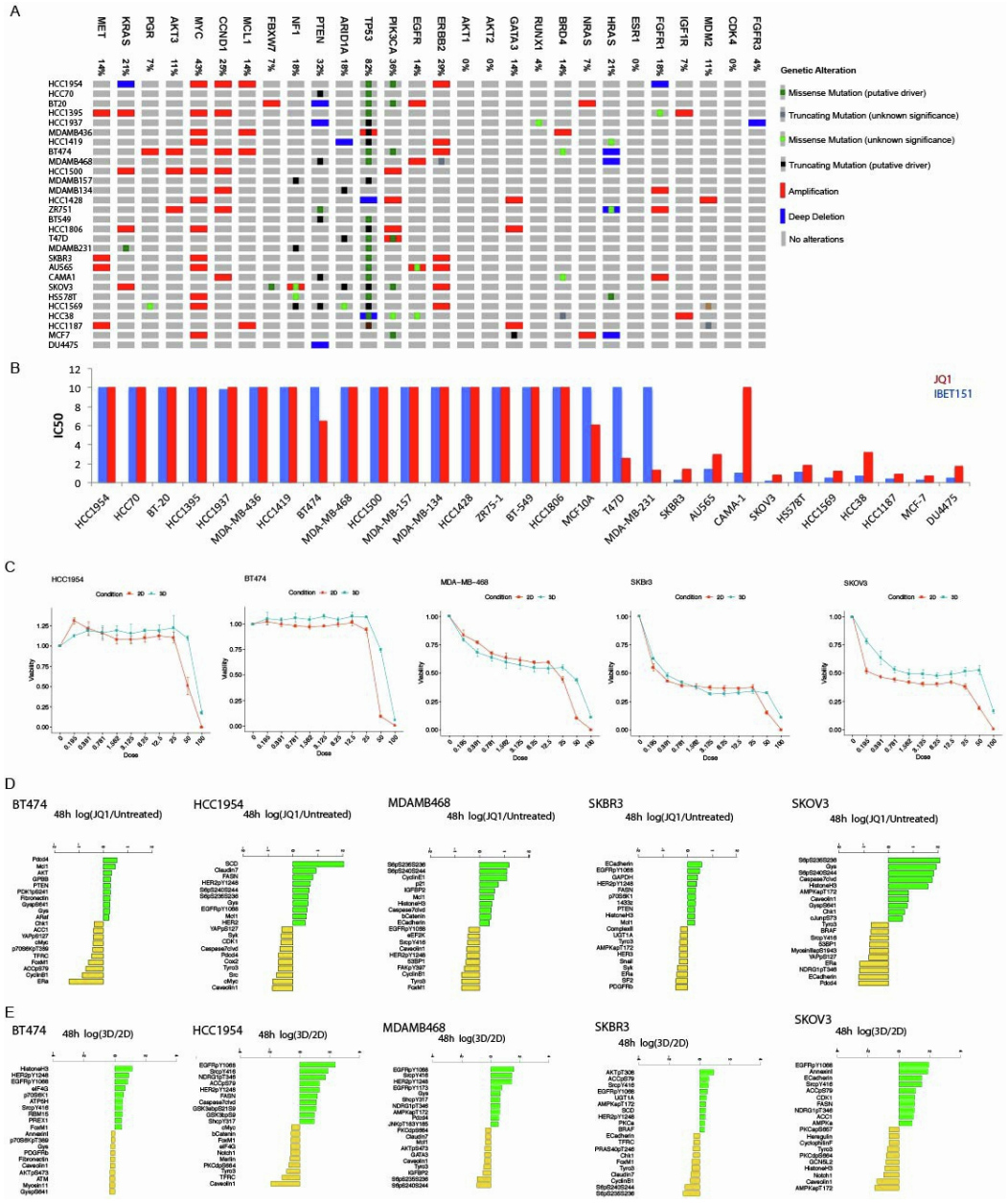

Figure S1. Genomic and BETi response diversity in breast cancer. Related to Figure 1. A. *Genomic alteration profiles in the breast cancer and ovarian (SKOV3) cell lines treated with BETis. The order of cell lines reflects JQ1 sensitivity rank (top: most resistant, bottom: most sensitive). Genes that are frequently altered in breast cancer are included in the analysis.* ***B.*** *BETi (JQ1 and IBET151) cell viability response IC50 for cell lines.* ***C.*** *Dose response curves of BET inhibition in HCC1954, BT474, MDAMB468, SKBR3, and SKOV3 cultured in 2D and 3D.* ***D.*** *The responses to BET inhibition (JQ1 at 48hrs). Substantial changes (X>1 in log2 space) are observed in SCD in HCC1954, phospho-S6 in MDAMB468 and SKOV3, CyclinE1 in MDAMB468, and Gys, HistoneH3 and capspase7 clvd in SKOV3.* ***E.*** *Comparison of proteomic responses to BETi (JQ1) in 3D cultures vs. 2D cultures in all cell lines. The bar plots display relative values of response to JQ1 with respect to the responses in monolayered cultures. Most substantial increases are in EGFR phosphorylation at Y1068 (up to 2.4 increase in all cell lines except SKOV3), HER2 phosphorylation at Y1248 (log-fold increase of 0.4 in SKBR3 to 1.4 in SKOV3), HistoneH3 levels (1.2 log2-fold increase in BT474) and SRC phosphorylation at Y416 (up to 2 log-fold increase in all cell lines). Most substantial reduction induced by ECM attachment were in S6 phosphorylation at S235/236 and S240/244 (~1 log2-fold decrease in SKBR3 and MDAMB468), caveolin (2 log2-fold decrease in HCC1954) and AMPK_pT172 (1.6 log-fold decrease in SKOV3). AKT phosphorylation at T308 was increased in SKBR3; E-cadherin and annexin were increased in SKOV3 upon ECM attachment. Interestingly, responses in lipid metabolism proteins such as FASN and ACC1 (total and phosphorylated state) were higher in 3D cultured HCC1954 and SKOV3 lines.*

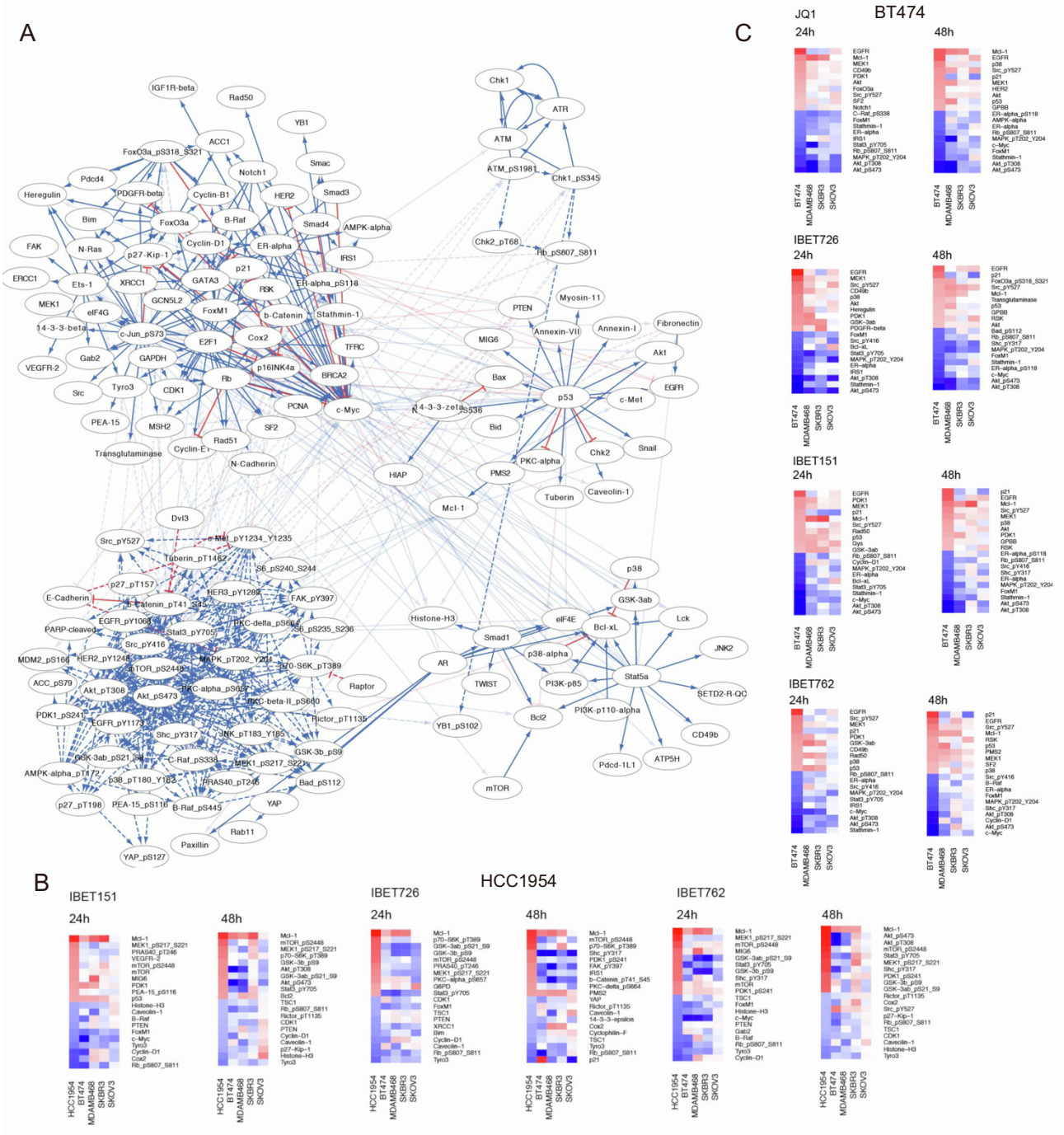

Figure S2. TargetScore analysis of cell lines treated with BETis, Related to Figure 2. *Positive TargetScores correspond to potential adaptive responses to perturbations. Negative TargetScores correspond to potential direct responses to a targeted agent (e.g., decrease in p-ERK in response to MEK inhibition).* ***A.*** *The reference network used in TargetScore calculations.* ***B****. The heatmaps of TargetScores calculated for each drug treatment in HCC1954 cells cultured in 3D cultures (JQ1 plot is in Figure 2). The cell lines are ordered from most resistant (HCC1954) to most sensitive (SKOV3). The proteins with 10 highest and 10 lowest TargetScores from HCC1954 are listed.* ***C.*** *Similar heatmaps as in (B) based on the top and bottom TargetScores for BT474 cells. Particularly in the HCC1954 and BT474, cell cycle proteins RB1_pS807, CyclinD1, c-Myc, and p27/Kip1 had the lowest TargetScores. Our differential and statistical analyses of TargetScores suggest that BETis reduce cell cycle progression as indicated by low TargetScores in cell cycle pathways. Interestingly, in BT474, phosphorylation of MAPK and AKT pathway members were also marked with low TargetScores despite increases in total proteins levels and corresponding high TargetScores of total protein expression in EGFR, AKT and MAPK pathway members, suggesting BRD4 inhibitors alter signaling processes downstream of EGFR/HER2 in BT474.*

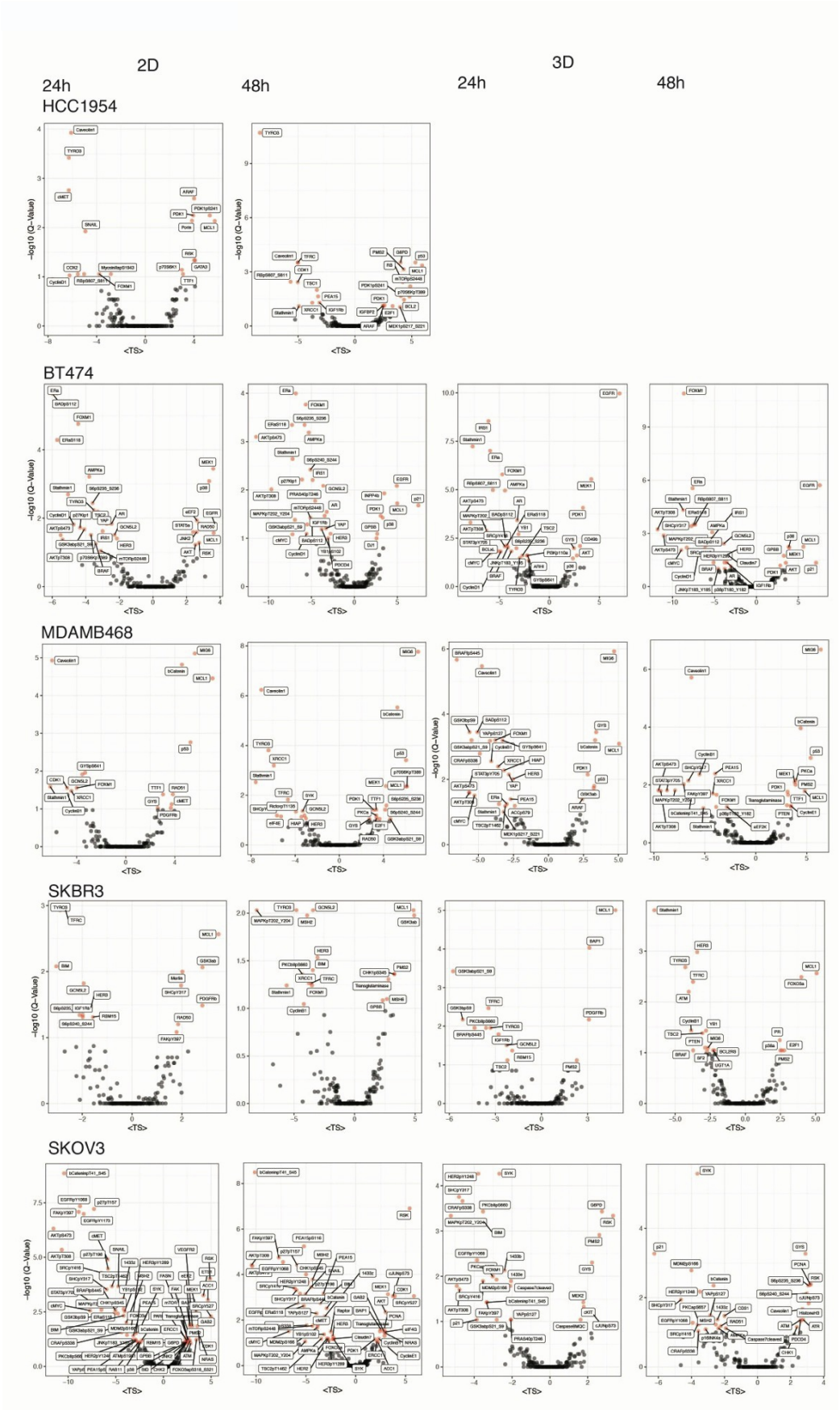

Figure S3. The statistical assessment of TargetScores, Related to Figure 2. *The volcano plots list the statistically most significant scores (FDR adjusted Q values on y-axis) and highest average TargetScores across 4 BETis (<TS> in x-axis). The results are given for both 2D and 3D cultured cells for all cell lines analyzed at 24h and 48h.*

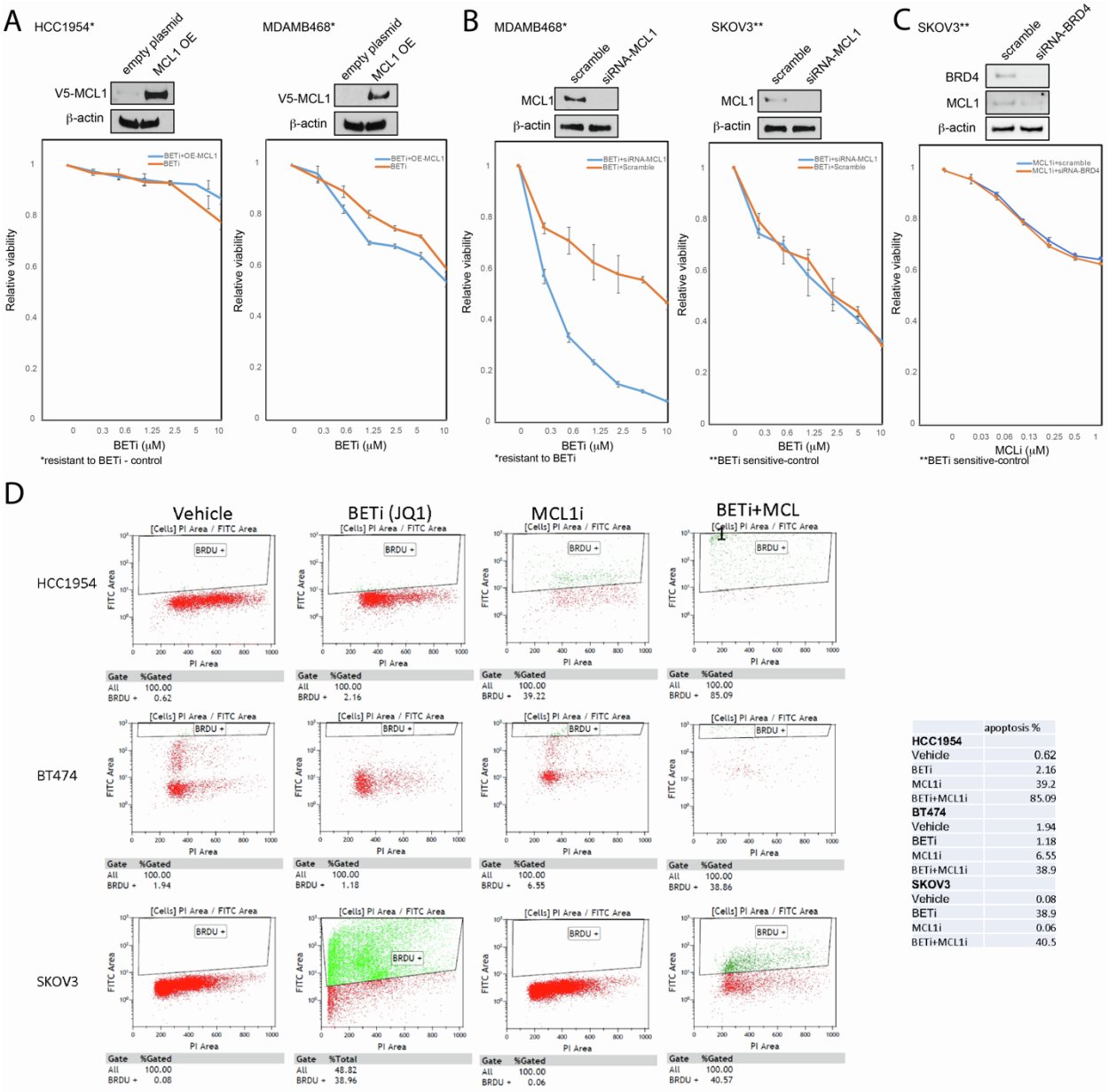

	apoptosis %
HCC1954	
Vehicle	0.62
BETi	2.16
MCL1i	39.2
BETi+MCL1i	85.09
BT474	
Vehicle	1.94
BETi	1.18
MCL1i	6.55
BETi+MCL1i	38.9
SKOV3	
Vehicle	0.08
BETi	38.9
MCL1i	0.06
BETi+MCL1i	40.5

Figure S4. ***Overexpression and knockdown of BRD4 and MCL1, Related to Figure 3.*** ***A.*** *Overexpression (OE) of MCL1 in already resistant HCC1954 and MDAMB468 cells does not further increase the resistance to BETi in contrast to OE of MCL1 in the sensitive SKOV3 cells (Figure 3D). The western blots with V5-tag antibody confirm MCL1 OE with detection of V5-tagged MCL1 (top). The cell viability responses to BETi in wild-type vs. MCL1 overexpressing HCC1954 and MDAMB468 cells (bottom). The error bars represent +/-SEM over 4 replicates.* ***B****. MCL1 knockdown (KD) in MDAMB468 and SKOV3. The western blots confirm the KD (top). The cell viability responses to BETi in MDAMB468 (BETi resistant) and SKOV3 (BETi sensitive) after MCL1 KD with siRNA. In MDAMB468 as well as HCC1954 (Figure 3E), MCL1 KD sensitizes cells to BETi. In SKOV3 cells with already low MCL1, BETi sensitivity remains unchanged with MCL1 is KD.* ***C****. BRD4 KD. The western blots confirm KD of BRD4 induces MCL1 expression consistent with the effect of BETi (top). The BRD4 KD and MCL1i inhibition cell viability responses (bottom). MCL1 and BRD4 KD in SKOV3 does not alter responses to MCL1 inhibitor as MCL1-levels are intrinsically low in SKOV3 cells and cells are refractory to MCL1 inhibition.* ***D.*** *Apoptotic responses to MCL1i (0.3 μM S63845) and BETi (2 μM JQ1) 48-hours post-treatment in HCC1954, BT474 and SKOV3 are measured with flow cytometry-based BRDU assay to quantify DNA double stranded breaks and total DNA content.*

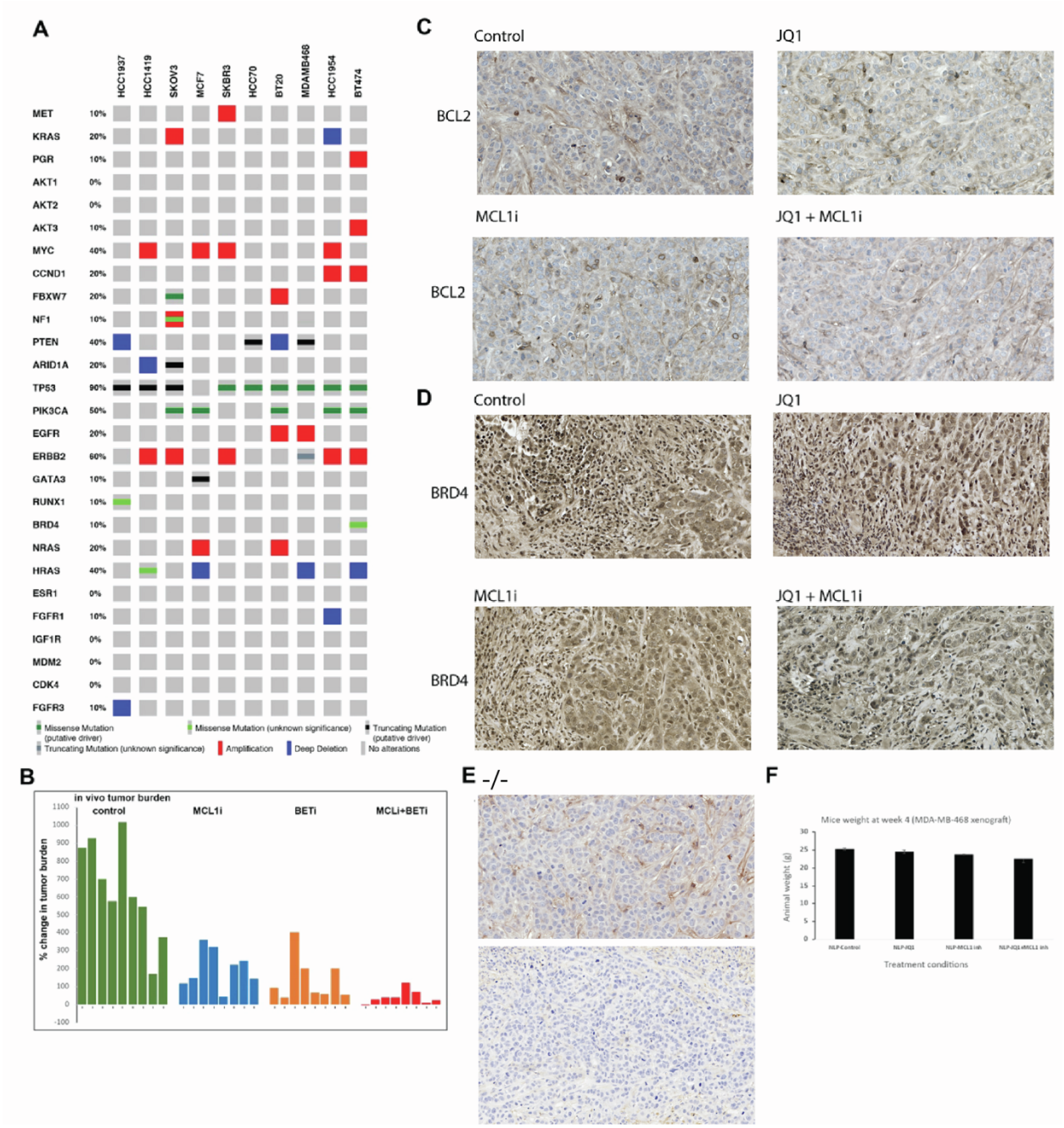

Figure S5. The genomic, histological and pharmacological characterization of BETi responses in cell lines and xenografts, Related to Figure 4. A. *The genomic alterations in the breast and ovarian (SKOV3) cell lines tested with the BET and MCL1 inhibitor combination.* ***B.*** *The tumor burden change in control and drug treatment (BETi, MCL1i, combination) in MDAMB468 xenograft model. N=9/arm for control, N=8/arm for treatment cohort. One animal was sacrificed for IHC analyses and excluded from analysis.* ***C.*** *Representative images of immunohistochemical analysis of BCL2 expression in MCL1 and BET inhibitor treated tumor xenograft models.* ***D.*** *Representative images of immunohistochemical analysis of BRD4 expression in drug treated tumor xenograft models.* ***E.*** *The negative control IHC stainings with no primary antibody treatment. Top: Negative control for figure 5G, S5C, S5D. Bottom: Negative control for figure 4H-I.* ***F.*** *Animal weights in each condition at the termination time of the experiment.*

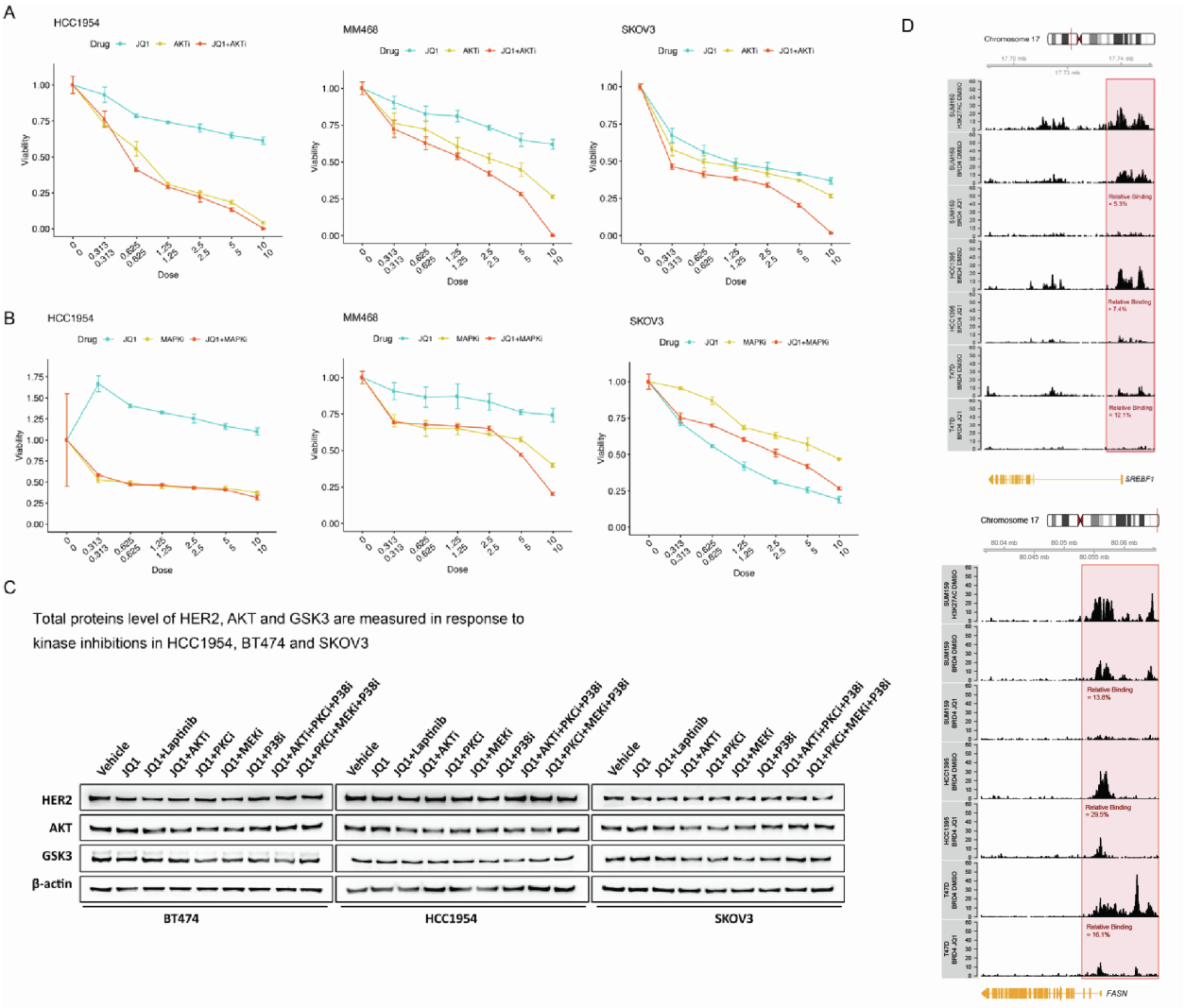

Figure S6. The characterization of BETi response mechanisms in breast cancer cell cells, Related to Figure 5. *The cell viability response to combination of BET inhibitors with **A**. AKT inhibitor, **B.** MEK1/2 inhibitors (trametinib). **C**. HER2, AKT, GSK3 total protein levels in response to pathway and BET inhibitors in HCC1954, BT474 and SKOV3 are measured. The measurements of total proteins demonstrate the total protein levels are not changed and observed phosphorylation changes (Figure 5C) are due to signaling changes and not due to changes in the total levels. **D**. ChIP-seq Analysis of BRD4 binding on SREBF1 (top) and FASN (bottom) gene regulatory sites in breast cancer cell lines treated with BET inhibitors (JQ1). The H3K27ac antibody binding sites mark the active promoter regions for the SREBF1 and FASN genes. The ChIP-seq with BRD4 antibody marks the binding of BRD4 to SREBF1 and FASN promoter regions and BRD4 removal by BET inhibition (Original data GEO: GSE63581).*

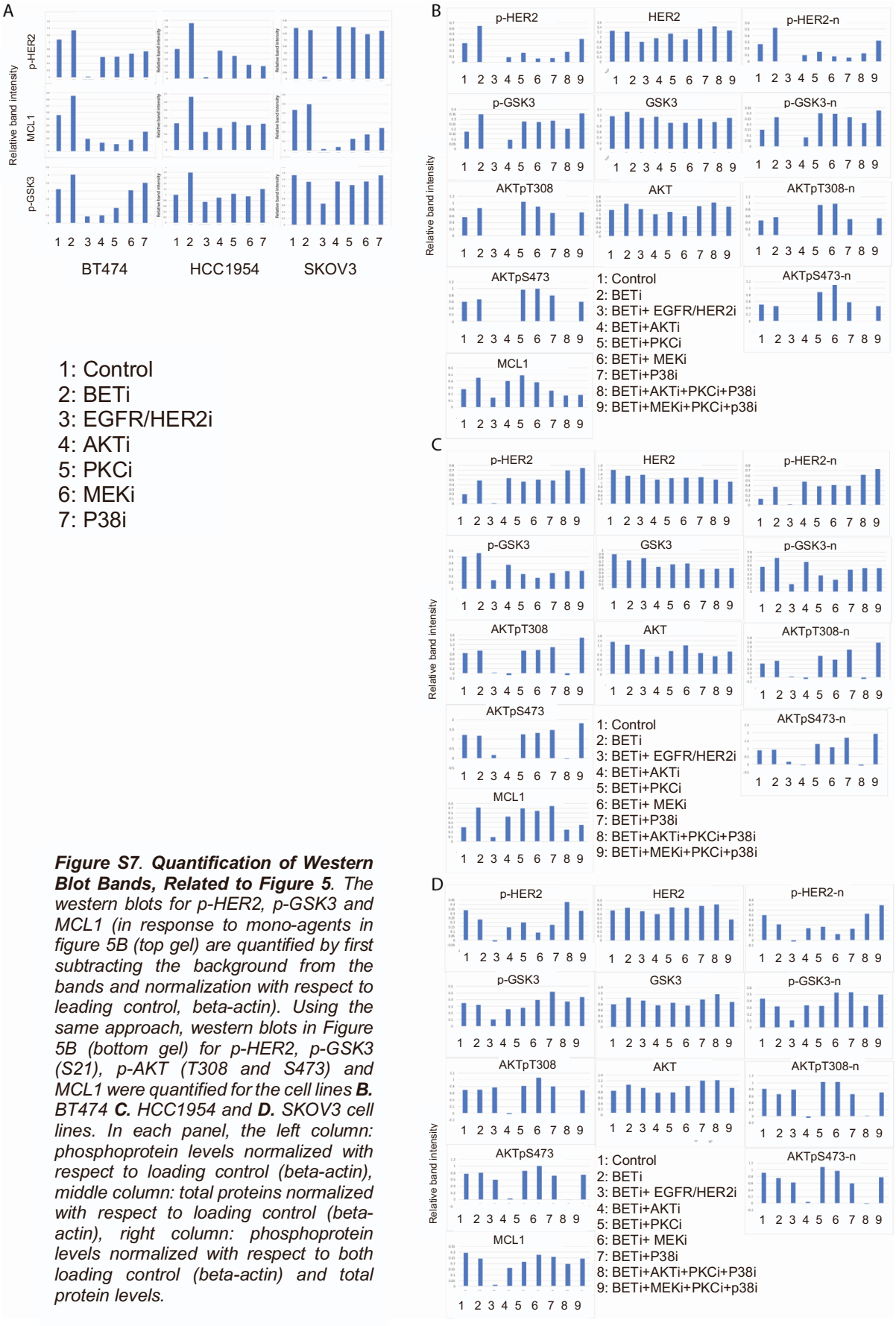

Figure S7. Quantification of Western Blot Bands, Related to Figure 5*. The western blots for p-HER2, p-GSK3 and MCL1 (in response to mono-agents in figure 5B (top gel) are quantified by first subtracting the background from the bands and normalization with respect to leading control, beta-actin). Using the same approach, western blots in Figure 5B (bottom gel) for p-HER2, p-GSK3 (S21), p-AKT (T308 and S473) and MCL1 were quantified for the cell lines* ***B.*** *BT474* ***C.*** *HCC1954 and* ***D.*** *SKOV3 cell lines. In each panel, the left column: phosphoprotein levels normalized with respect to loading control (beta-actin), middle column: total proteins normalized with respect to loading control (beta-actin), right column: phosphoprotein levels normalized with respect to both loading control (beta-actin) and total protein levels.*